**RESEARCH ARTICLE**

# The α5-nAChR/PD-L1 axis facilitates lung adenocarcinoma cell migration and invasion

Ping Zhu[1] · Guiyu Kang[1] · Yang Jiao[2] · Chengzhi Gui[3] · Huiping Fan[3] · Xiangying Li[2] · Yanfei Jia[3] · Lulu Zhang[3] · Xiaoli Ma[1,2,3]

## Abstract

α5 nicotinic acetylcholine receptor (α5-nAChR) is associated with the progression of smoking-related lung adenocarcinoma (LUAD), but the molecular mechanism is unclear. Programmed death ligand 1 (PD-L1) is encoded by the CD274 gene, which not only inhibits the immune system, but also plays a unique role in tumor growth and metastasis. Here, we gained important insights into the underlying mechanism between α5-nAChR and PD-L1 in LUAD progression. α5-nAChR was overexpressed in various histological subtypes, cancer stages and metastasis statuses of LUAD. The group that coexpressed α5-nAChR and PD-L1 had a worse prognosis than the other subgroups at different stages of LUAD lymph node metastasis. The expression of α5-nAChR and PD-L1 was associated with epithelial–mesenchymal transition (EMT) marker CDH2. In vitro, α5-nAChR mediated nicotine-induced PD-L1 expression via STAT3 and the expression of EMT markers. Downregulation of α5-nAChR and/or PD-L1 inhibited EMT marker expression, cell proliferation, migration and invasion compared to silencing α5-nAChR or PD-L1 alone in LUAD cells. Furthermore, α5-nAChR expression was associated with PD-L1 and EMT marker expression in mouse xenograft models. These results highlight that α5-nAChR mediates STAT3/PD-L1 signaling, which contributes to cell migration and invasion. Therefore, our study may reveal a new interaction between α5-nAChR and PD-L1 that is involved in tumor cell growth and progression in LUAD, which may be a promising target for NSCLC diagnosis and immunotherapy.

**Keywords** α5 nicotinic acetylcholine receptor · STAT3 · PD-L1 · Epithelial–mesenchymal transition · Lung adenocarcinoma

## Introduction

According to the latest cancer statistics, lung cancer is the leading cause of death worldwide [1, 2]. Tobacco dependence is associated with higher lung cancer and mortality rates [3]. Non-small cell lung cancer (NSCLC) represents approximately 85% of lung cancers [4]. Effective progress in treatment options, including surgery, radiotherapy, chemotherapy, targeted therapy, and immunotherapy, remains poor,

as the majority of patients have locally advanced or extensively metastatic tumors at diagnosis [5]. Epithelial–mesenchymal transition (EMT) is generally considered to be the key to promoting lung cancer metastasis [6, 7]. Therefore, it is necessary to elucidate the molecular mechanism of EMT in lung cancer progression.

Nicotinic acetylcholine receptors (nAChRs) are membrane ligand-gated ion channels that are present throughout the central nervous system and in nonneuronal tissues, such as bronchial epithelium, alveolar epithelial cells, pulmonary neuroendocrine cells, skin keratinocytes, vascular tissues, and human lymphocytes [8]. Research in recent years has shown that activation of nicotine/nAChR signaling is associated with lung cancer risk [9–12]. Notably, genome-wide association studies (GWAS) have shown that variations in the α3, β4, and α5 subunit regions encoding nAChRs are strongly associated with nicotine dependence and lung cancer [13, 14]. Our previous study reported that α5-nAChR contributes to lung cancer development and progression

✉ Xiaoli Ma
  Maxiaoli_jn@sdu.edu.cn

1   Department of Medical Laboratory, Weifang Medical University, Weifang 261053, China

2   Jinan Central Hospital, Shandong University, Jinan 250013, China

3   Research Center of Basic Medicine, Central Hospital Affiliated to Shandong First Medical University, Jinan 250013, China

via STAT3 signaling [15–17]. However, the mechanism by which $\alpha$5-nAChR promotes NSCLC metastasis is not fully understood.

Programmed cell death protein 1 (PD-1, encoded by CD279) is one of the coinhibitory receptors that is expressed on the surface of antigen-stimulated T cells [18]. PD-1 interacts with two ligands, PD-L1 (CD274) and PD-L2 (CD273). PD-L1 expression can be detected on hematopoietic cells and nonhematopoietic healthy tissue cells. Both PD-L1 and PD-L2 can be expressed by the tumor stroma [19]. PD-L1 is more effective than PD-L2 at inhibiting T cell activation [20]. PD-1/PD-L1 transmits negative regulatory signals to immune cells to maintain immune tolerance and suppress autoimmunity [21]. Recent studies have demonstrated that increased PD-L1 expression is an unfavorable prognostic factor for NSCLC and that PD-L1 expression is associated with smoking status [22]. Several recent studies have shown that advanced NSCLC patients with positive PD-L1 expression are more likely to respond to anti-PD-1 monotherapy than those who have never smoked [23–25]. PD-L1 not only plays roles in the suppression of the immune system, but also has distinct tumor-intrinsic roles in growth, metastasis, and resistance to therapy [26]. Furthermore, studies have shown that nicotine-induced $\alpha$9-nAChR activity promotes PD-L1 upregulation and melanoma cell proliferation and migration [27]. In addition, $\alpha$7-nAChR induces the STAT3/NRF2 pathway and promotes the expression of PD-L1 in normal lung epithelial cells [28]. However, it is still unclear whether $\alpha$5-nAChR and PD-L1 have an internal relationship in lung cancer metastasis.

In the present study, we examined $\alpha$5-nAChR and PD-L1 expression and demonstrated that $\alpha$5-nAChR expression was positively associated with PD-L1 in vitro and in vivo. Furthermore, $\alpha$5-nAChR mediated LUAD cell proliferation, migration and invasion via STAT3/PD-L1 signaling. Our findings provide new insights into the roles of $\alpha$5-nAChR and PD-L1 in NSCLC development and provide potential targets for NSCLC treatment.

## Methods

### Bioinformatics analysis

The GEPIA online database (http://gepia2.cancer-pku.cn/) was used to analyze the expression of different subunits of alpha nAChRs in NSCLC patients. Expression patterns of CHRNA5 in LUAD based on individual cancer stages and nodal metastasis status were analyzed using the UALCAN database (http://ualcan.path.uab.edu/index.html). The association of CHRNA5 and CD274 expression with CDH2 (encoding N-cadherin protein) was obtained using TIMER (https://cistrome.shinyapps.io/timer/). The gene expression of $\alpha$5-nAChR and PD-L1 data were obtained from the cancer genomic browser of UCSC Xena (https://xenabrowser.net/) to test the prognostic value of high coexpression of CHRNA5 and CD274 in different LUAD stages of lymph node metastasis.

### Cell culture

The human NSCLC cell lines A549 and H1299 were purchased from the Cell Resource Center of the Chinese Academy of Sciences. All NSCLC cells were grown in RPMI 1640 (HyClone, USA) with 10% fetal bovine serum (Gibco, USA) and 1% penicillin–streptomycin liquid (Macgene, China) in a 37 °C, 5% $CO_2$ incubator. NSCLC cell lines were treated with 1 μM nicotine (Sigma, USA) for 16 h as described in our previous study [29].

### Small interfering RNA (siRNA) transfection

The siRNAs for CHRNA5, CD274 and the negative control were obtained from RiboBio (China). A549 or H1299 cells were plated in six-well plates, when cells reached 60–70% confluence, the siRNAs were added to a final concentration of 15 nM with Lipofectamine 2000 (Invitrogen, USA) according to the manufacturer's instructions. The sequences of small interfering RNA were as follows: si-CHRNA5 5′-GGTCCGCAAGATATTTCTT-3′, si-CD274 5′-GCTGAA TTGGTCATCCCAG-3′.

### Western blotting

Total cell protein extracts were obtained in RIPA lysis buffer (Beyotime, China) according to the manufacturer's instructions. For Western blotting analysis, total protein was separated on a 10% SDS-PAGE gel and transferred onto nitrocellulose membranes (0.45 μm, Millipore, USA), which were then incubated at 4 °C overnight. The following antibodies were used: $\alpha$5-nAChR (1:800, GeneTex, Cat. No. GTX55490), pSTAT3 (1:2000, CST, Cat. No. 9145), STAT3 (1:2000, CST, Cat. No. 4904), PD-L1 (1:5000, Proteintech, Cat. No. 66248-1-Ig), Zeb1 (1:2000, Proteintech, Cat. No. 21544-1-AP), N-cadherin (1:1000, ABclonal, Cat. No. A19083), Vimentin (1:5000, Proteintech, Cat. No. 10366-1-AP), Snail1 (1:1000, Proteintech, Cat. No. 13099-1-AP), and GAPDH (1:10,000, Proteintech, Cat. No. 10494-1-AP). Horseradish peroxide-conjugated secondary antibodies were obtained from Proteintech Group, Inc. (1:10,000).

### Chromatin immunoprecipitation (ChIP) assay

A SimpleChIP® Plus Kit (9004S, CST) was used to perform the ChIP assay. Briefly, the cells were fixed with formaldehyde and then lysed. An anti-STAT3 antibody or normal IgG

was used to precipitate the DNA fragments (1:2000, CST, Cat. No. 4904). The DNA–protein complexes were pulled down with agarose beads and then decross-linked. The extracted DNA samples were then amplified by real-time PCR using primers targeting the PD-L1 promoter, which has been shown to interact directly with STAT3 [27].

## CCK-8 assay

A total of 3500 A549 or H1299 cells per well were plated in 96-well plates. After the cells adhered, they were transfected with si-NC, si-CD274 or si-CHRNA5. The cell proliferation assay was performed with the addition of 10 μL CCK-8 solution (Elabscience, China) into each well, followed by incubation at 37 °C for 1 h. Cell viability was analyzed by a microplate reader at a wavelength of 450 nm.

## Wound-healing assay

Cell migration was evaluated by wound-healing assay. Briefly, $2 \times 105$ A549 or H1299 cells per well were seeded in six-well plates. After the cells grew to approximately 90% confluence, the cell monolayers were wounded vertically with a 20 μL or 200 μL sterile pipette tip. The wells were washed with PBS, and fresh medium was added. Migrated cells were observed and captured 0 and 24 h after scratching using an Olympus CKX41 microscope.

## Cell migration and invasion assay

The cell migration assay was conducted using 24-well plates with 8-μm pore Transwell chambers (Corning, USA). A total of $1 \times 105$ A549 or H1299 cells were placed in the upper chambers in serum-free medium. The lower chamber was filled with culture medium containing 20% FBS. After 24 h, the nonmigrated cells were removed with clean swabs, and the cells on the bottom surface were stained with 0.1% crystal violet dye.

For the cell invasion assay, A549 or H1299 cells were seeded at a density of $1 \times 105$ cells/well in the upper chamber filled with Matrigel (Corning, USA). After 24 h, the noninvaded cells were removed with swabs, and the cells on the underside were stained with 0.1% crystal violet dye. A549 or H1299 cell migration and invasion were quantified using an inverted-contrast microscope.

## Xenograft tumor model

The animal assays were approved by the Institutional Animal Care and Use Committee of Central Hospital Affiliated to Shandong First Medical University. BALB/c nude mice (4–6 weeks old) were used in vivo studies. To induce ectopic tumor formation, a total of $2 \times 10^6$ A549 cells stably suppressing CHRNA5 or control cells were injected into nude mice subcutaneously. Tumors were evaluated every 3 days, and the volume was calculated by the following formula: $length \times width^2/2$. At the end of the experiment, mice were killed by cervical vertebra dislocation. Paraffin sections of lung tumor xenografts were obtained from our laboratory [30].

## Immunohistochemistry (IHC) analysis

IHC assays to examine the expression of *α*5-nAChR, PD-L1 and EMT markers in the tumor xenografts were performed on sections (4 μm thickness) using a biotin assay system (Beijing Zhongshan Jinqiao, China, Cat. No. PV-9001, PV-9002) following the manufacturer's instructions. The samples on the slides were incubated at 4 °C overnight with a mouse monoclonal antibody against *α*5-nAChR (1:200, Proteintech, Cat. No. 66363-1-Ig), a mouse monoclonal antibody against PD-L1 (1:500, Proteintech, Cat. No. 66248-1-Ig), a rabbit antibody against N-cadherin (1:100, ABclonal, Cat. No. A19083), and a rabbit polyclonal antibody against Snail1 (1:100, Proteintech, Cat. No. 13099-1-AP). For IHC analysis, the grading was as follows: not dyed was scored as 0, yellow was scored as 1, and brown was scored as 2. A percentage of positive tumor cells in the visual field $< 1\%$ was scored as 0, while 1–25% was scored as 1, 25–75% was scored as 2, and 75–100% was scored as 3. The final score was determined by multiplying the intensity score by the proportion of positive cells.

## Statistical analysis

All data were analyzed and graphed using GraphPad Prism 7.0 or SPSS v23.0. The experimental data are presented as the means $\pm$ SD. A two-group comparison was analyzed by Student's *t* test, and multiple group comparison was analyzed by one-way ANOVA + two-side Dunnett test or one-way ANOVA + two-side Tukey test. The survival analysis was performed by Kaplan–Meier curve. *P* value $< 0.05$ was considered statistically significant.

# Results

## *α*5-nAChR expression levels and correlations with clinicopathological parameters in multiple databases

To evaluate the expression of nAChR subunits in lung cancer, we retrieved the mRNA levels of alpha nAChR subunits from the GEPIA database. The expression of CHRNA5 was more prominent than that of the other alpha nAChR subunits (Fig. 1A). We used the UALCAN online database
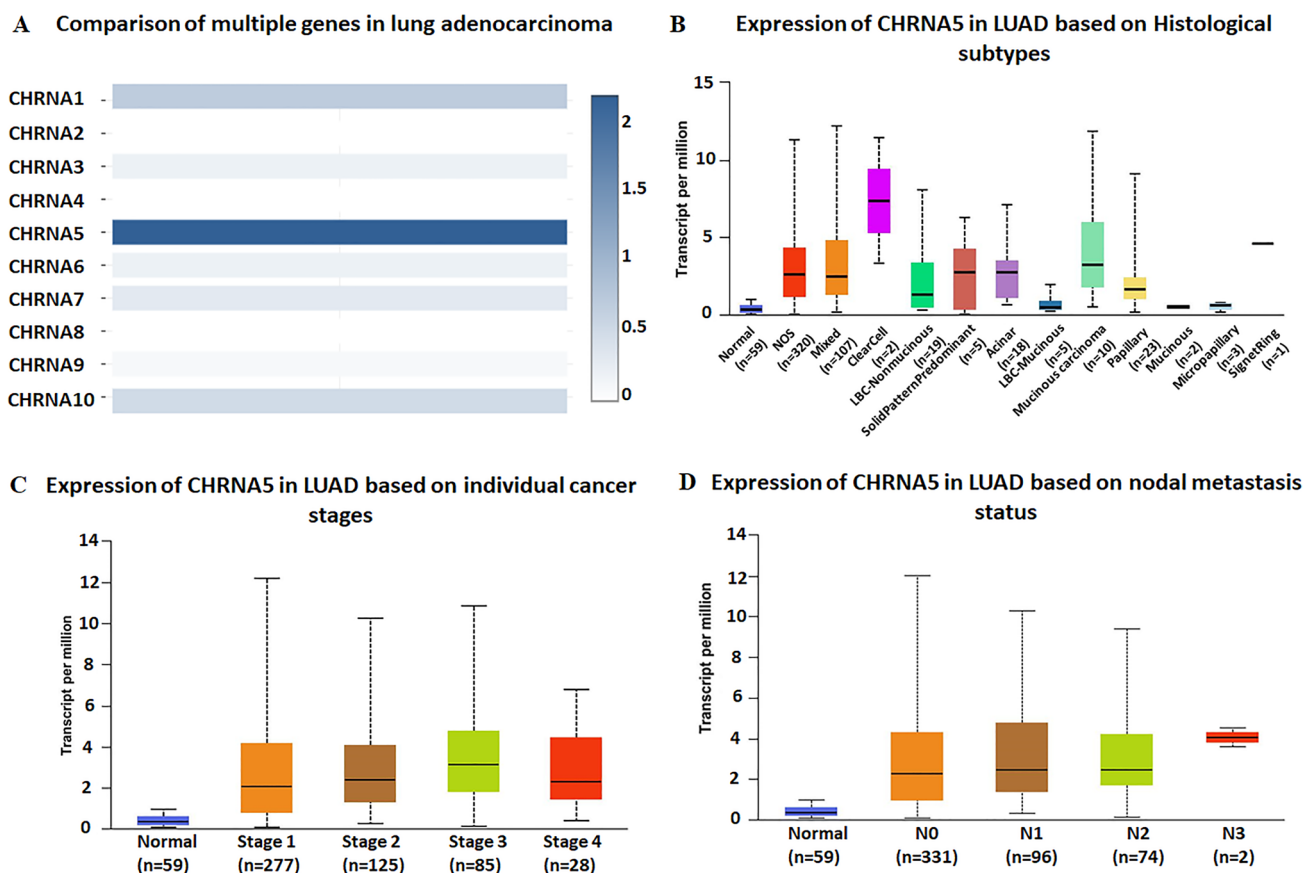
**A  Comparison of multiple genes in lung adenocarcinoma**



**B  Expression of CHRNA5 in LUAD based on Histological subtypes**



**C  Expression of CHRNA5 in LUAD based on individual cancer stages**



**D  Expression of CHRNA5 in LUAD based on nodal metastasis status**



**Fig. 1** CHRNA5 expression in multiple databases. **A** Comparison of multiple genes in lung adenocarcinoma. **B** The expression of CHRNA5 based on histological subtypes in LUAD. **C** The expression of CHRNA5 based on individual cancer stages in LUAD. **D** The expression of CHRNA5 based on nodal metastasis status in LUAD

to investigate the relationships between CHRNA5 and clinicopathological parameters. The results showed that CHRNA5 expression levels were significantly higher in various histological subtypes of LUAD ($n = 515$) than in the normal tissues ($n = 59$, Fig. 1B), especially in NOS, mixed, LBC-nonmucinous, acinar, mucinous, and papillary LUAD ($P < 0.05$). A high expression of CHRNA5 was significantly correlated with clinical stage 1–2 ($P < 0.05$, Fig. 1C) and an N0–N1 lymph node status ($P < 0.05$, Fig. 1D) in LUAD. These results suggested that $\alpha$5-nAChR correlates with lymph node metastasis status and clinical stage.

## Expression of CHRNA5 and CD274 correlates with poor prognosis and CDH2 in LUAD patients in the TCGA dataset

Several clinical trials have reported that smoking status influences overall survival (OS) in anti-PD-1/PD-L1-treated lung cancer patients [31]. However, the effect of CHRNA5 and CD274 coexpression on patient OS in metastatic lung adenocarcinoma remains unclear. To further test the

prognostic value of the high coexpression of CHRNA5 and CD274 in metastatic LUAD, we downloaded $\alpha$5-nAChR and PD-L1 gene expression data from UCSC Xena. The survival time was lower for patients with high CHRNA5 and CD274 coexpression than for those with a high expression of CHRNA5 or CD274 alone or with a low coexpression in stage N0 of lung adenocarcinoma (Fig. 2A). Similar results were observed among stage N1 LUAD patients (Fig. 2B). Interestingly, there was a positive correlation between CDH2 and CHRNA5 or CD274 from the TIMER online database (Fig. 2C, D). This result suggested that CHRNA5 and CD274 may correlate with metastasis in LUAD.

## Nicotine activates pSTAT3, PD-L1 and EMT marker expression via $\alpha$5-nAChR signaling in NSCLC cells

The expression of $\alpha$5-nAChR, PD-L1, pSTAT3, Zeb1, N-cadherin, Vimentin and Snail1 was upregulated in A549 and H1299 cells treated with 1 $\mu$M nicotine for 16 h (Fig. 3A, B). In addition, the results showed that the expression of PD-L1, pSTAT3, Zeb1, N-cadherin, Vimentin and
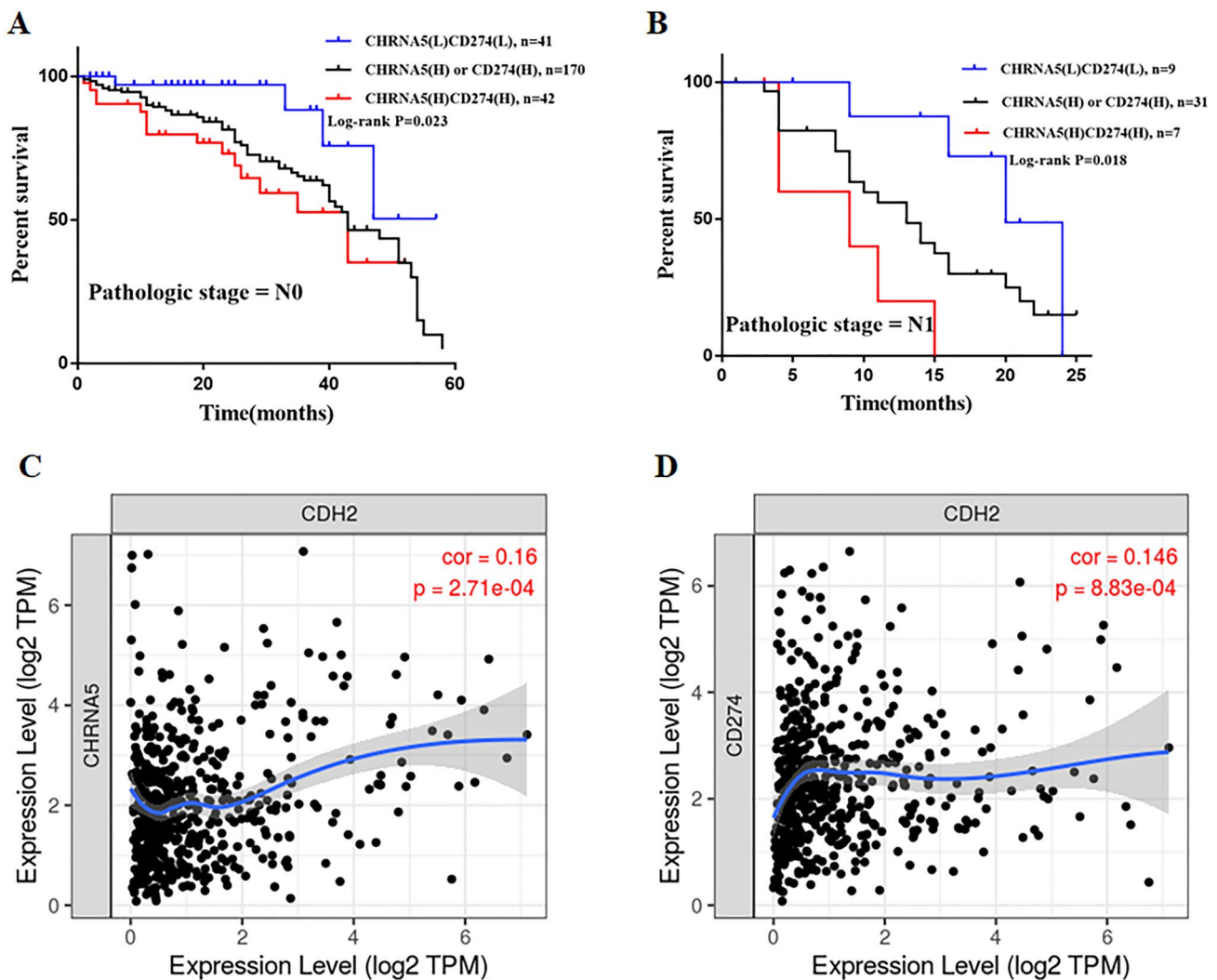
**Fig. 2** Expression of CHRNA5 and CD274 correlates with poor prognosis and CDH2 in LUAD. **A** Coexpression of CHRNA5 and CD274 had a worse prognosis than the expression of either alone or low coexpression in stage N0 LUAD. **B** Coexpression of CHRNA5 and CD274 had a worse prognosis than the expression of either alone or low coexpression in stage N1 LUAD. **C** The association of CHRNA5 expression with CDH2 in LUAD. **D** The association of CD274 expression with CDH2 in LUAD

Snail1 was downregulated in the α5-nAChR-knockdown A549 and H1299 cells compared to the control cells (Fig. 3C, D). These results indicated that nicotine activates pSTAT3, PD-L1 and EMT marker expression via α5-nAChR signaling in NSCLC cells.

## α5-nAChR mediates PD-L1 expression via STAT3 by ChIP assay

Transcriptional element analysis (http://jaspar.genereg.net) revealed that the transcription factor STAT3 directly bound to the PD-L1 promoter at −337 to −118, as shown in Fig. 4A. We then performed a ChIP assay with an anti-STAT3 rabbit polyclonal antibody and primer pairs specific for the PD-L1 gene promoter in the si-CHRNA5 and si-NC group of H1299 cells. The results showed that PD-L1 expression was decreased by STAT3 binding to the PD-L1 promoter in the si-CHRNA5 group compared to the si-NC group (Fig. 4B). This result suggested that α5-nAChR mediates PD-L1 expression via STAT3.

## Downregulation of α5-nAChR and/or PD-L1 inhibits EMT marker expression in NSCLC cells

To investigate the interaction between α5-nAChR and PD-L1, a western blotting assay was used to detect the protein expression of pSTAT3, Zeb1, N-cadherin, Vimentin and Snail1 in the si-NC, si-CHRNA5, si-CD274 and si-CHRNA5 + si-CD274 groups. Silencing α5-nAChR decreased the levels of pSTAT3, PD-L1 and EMT markers
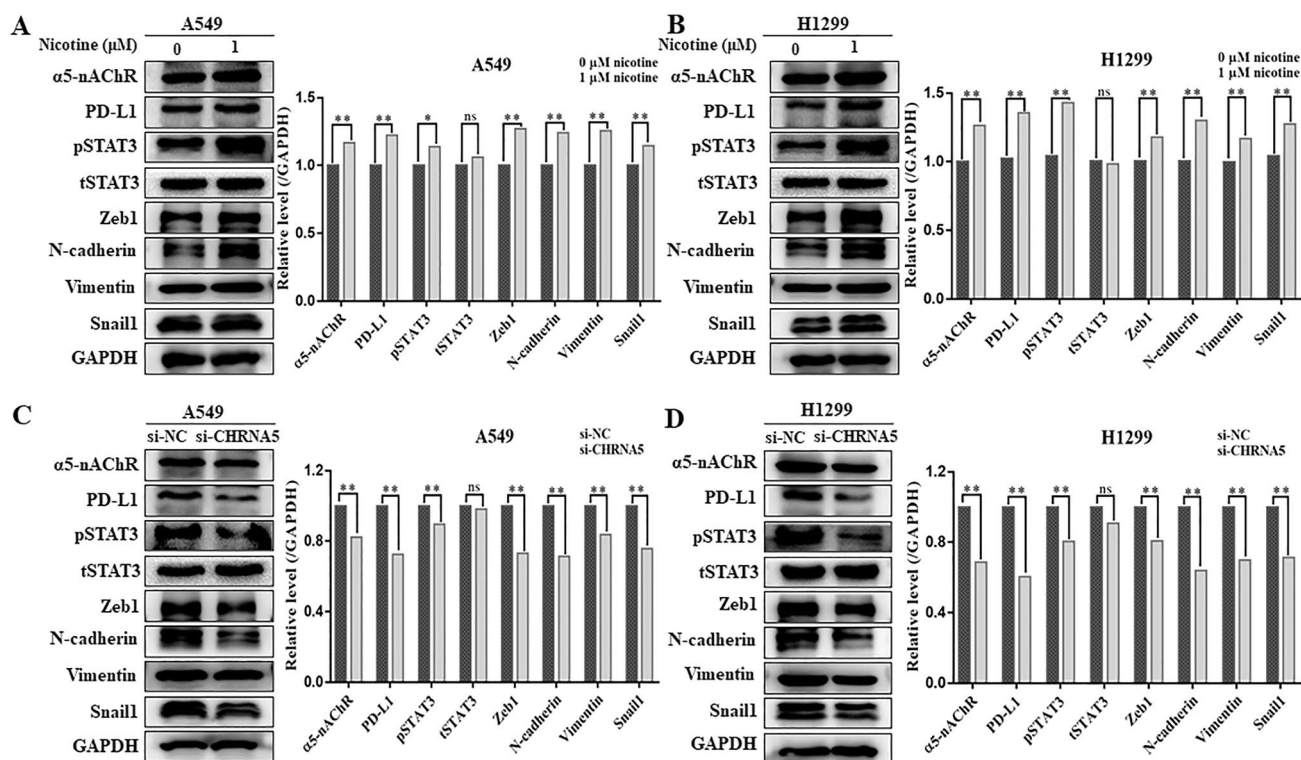
**Fig. 3** Nicotine activates PD-L1, pSTAT3 and EMT marker expression via α5-nAChR signaling in NSCLC cells. **A** Nicotine promoted expression of α5-nAChR, PD-L1, pSTAT3, Zeb1, N-cadherin, Vimentin and Snail1 in A549 cells. **B** Nicotine promoted expression of α5-nAChR, PD-L1, pSTAT3, Zeb1, N-cadherin, Vimentin and Snail1 in H1299 cells. **C** α5-nAChR silencing downregulated expres-
sion of PD-L1, pSTAT3, Zeb1, N-cadherin, Vimentin and Snail1 in A549 cells. **D** α5-nAChR silencing downregulated expression of PD-L1, pSTAT3, Zeb1, N-cadherin, Vimentin and Snail1 in H1299 cells. The data are presented as the mean ± SD of independent experiments; $n = 3$; *$p < 0.05$, **$p < 0.01$; *ns* not significantly different

in A549 and H1299 cells, which is generally consistent with the results of our previous study [16]. Moreover, silencing CD274 similarly decreased the levels of pSTAT3 and EMT markers. It is worth noting that compared to the si-CHRNA5 group and si-CD274 group, the expression of pSTAT3 and EMT markers was lower in the si-CHRNA5 + si-CD274 group in A549 (Fig. 4C) and H1299 cells (Fig. 4D). These results suggested that α5-nAChR mediates epithelia–-mesenchymal transition via the STAT3/PD-L1 pathway in NSCLC cells.

## α5-nAChR and/or PD-L1 expression mediates NSCLC cell proliferation, migration, and invasion

We then examined the effects of α5-nAChR and/or PD-L1 activity on cell proliferation in A549 and H1299 NSCLC cells for 24–48 h. As shown in Fig. 5A and B, we found that the combined interference with CHRNA5 and CD274 expression inhibited cell proliferation more significantly than interference of CHRNA5 or CD274 expression alone in a time-dependent manner in the two NSCLC cell lines.

Moreover, we performed wound-healing assays to examine the effects of α5-nAChR and/or PD-L1 on migration in A549 and H1299 cells. By comparing the migration areas at 0 h and 24 h, we found that the migration areas were significantly larger in the si-CHRNA5+si-CD274 group than in the si-CHRNA5 or si-CD274 group in A549 and H1299 cells (Fig. 5C, D).

The results of transwell assays ± Matrigel demonstrated that the downregulation of CHRNA5 or CD274 decreased cell migration and invasion compared to the si-NC group. Cell migration and invasion were significantly reduced in the si-CHRNA5 + si-CD274 group compared to the si-CHRNA5 group or si-CD274 group alone in A549 and H1299 cells (Fig. 6A, B).

## Expression of α5-nAChR, PD-L1, *N*-cadherin and Snail1 in NSCLC tumor xenografts

As α5-nAChR expression was verified to be associated with PD-L1 and EMT marker expression in NSCLC cell lines, we further assessed α5-nAChR, PD-L1, N-cadherin and Snail1 expression in LUAD xenograft tissues preserved by our
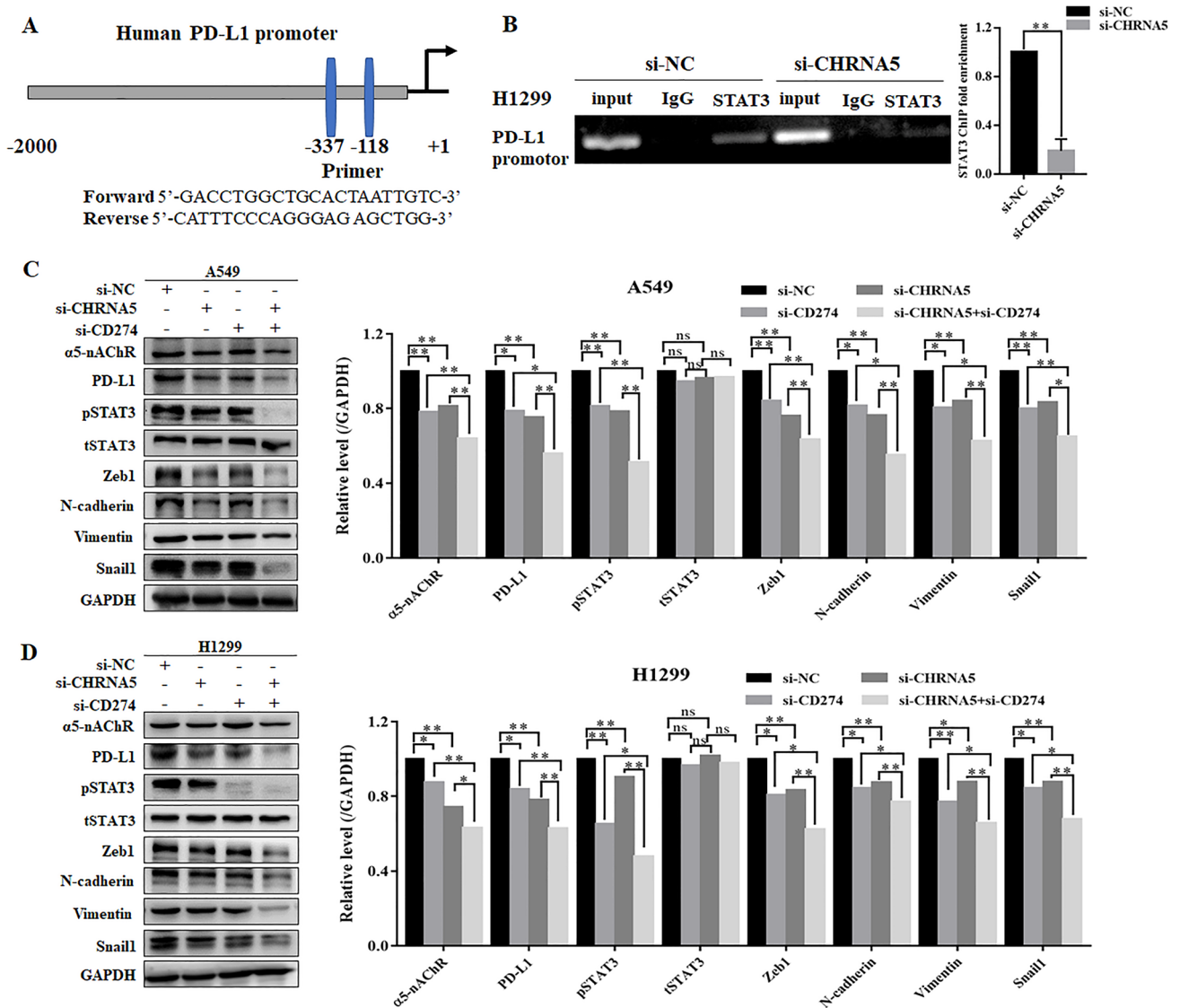
**Fig. 4** Downregulation of α5-nAChR and/or PD-L1 inhibits EMT marker expression in NSCLC cells. **A** The STAT3 binding site of the PD-L1 promoter. **B** ChIP assay showed that STAT3 bound to the PD-L1 promoter in H1299 cells. **C** α5-nAChR silencing and/or CD274 silencing downregulated expression of PD-L1, pSTAT3, Zeb1, N-cadherin, vimentin and Snail1 in A549 cells. **D** α5-nAChR silencing and/or CD274 silencing downregulated expression of PD-L1, pSTAT3, Zeb1, N-cadherin, vimentin and Snail1 in H1299 cells. The data are presented as the mean ± SD of independent experiments; $n = 3$; *$p < 0.05$, **$p < 0.01$; *ns* not significantly different

laboratory. The expression levels of α5-nAChR (Fig. 7A), PD-L1 (Fig. 7B), N-cadherin (Fig. 7C), and Snail1 (Fig. 7D) in the NC group were higher than those in the KD group. In addition, the expression of α5-nAChR, PD-L1, N-cadherin and Snail1 in nicotine-treated xenograft tissues was higher than that in the NC group. This result was also validated in the KD group and the nicotine-treated KD group. Together, these results suggested that α5-nAChR is associated with PD-L1, N-cadherin and Snail expression in vivo.
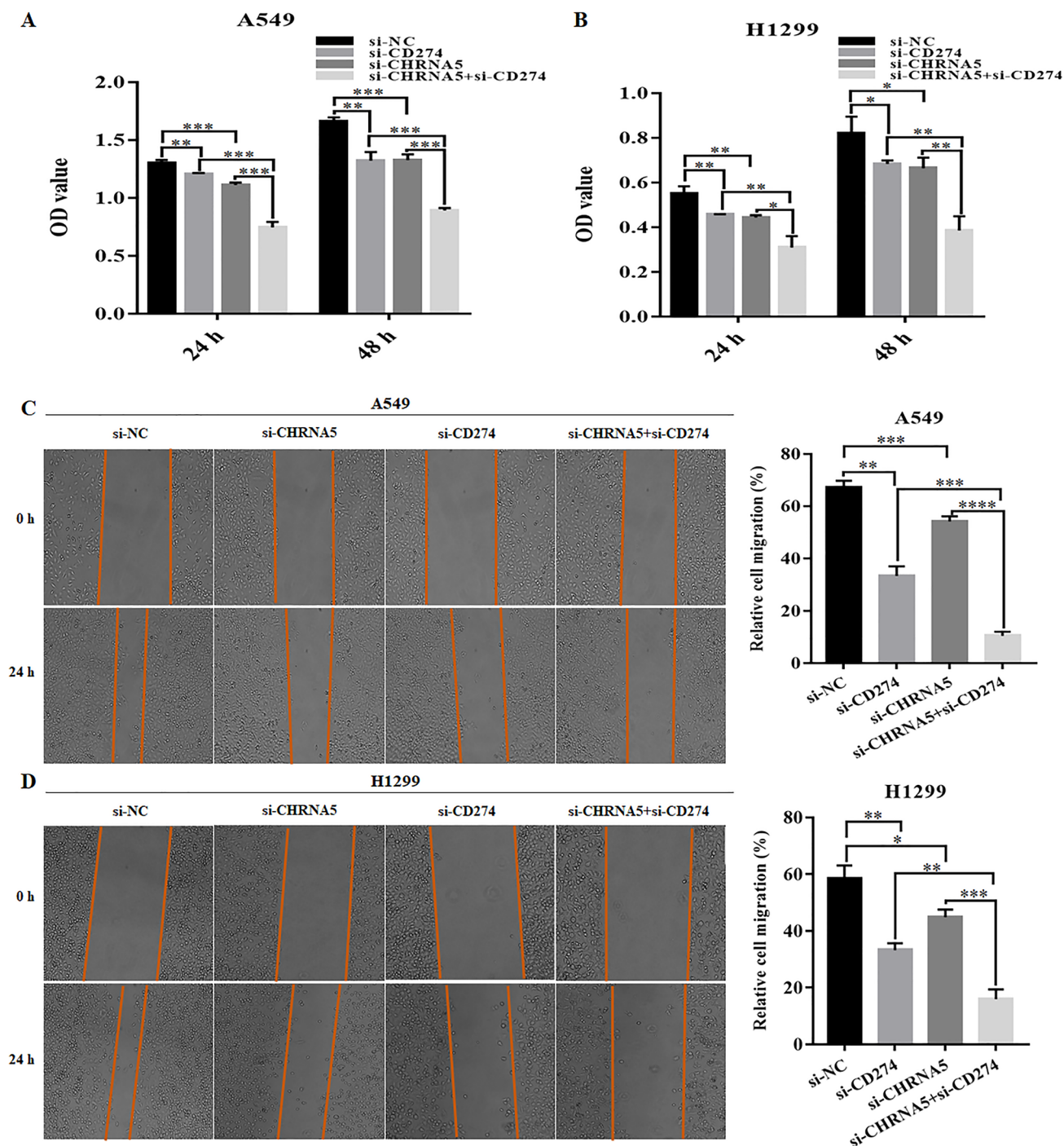
**Fig. 5** Inhibition of $\alpha$5-nAChR and/or PD-L1 affects lung cancer cell proliferation and migration. **A** CCK-8 assays showed that $\alpha$5-nAChR and/or PD-L1 downregulation inhibited the proliferation of A549 cells. **B** CCK-8 assays showed that $\alpha$5-nAChR and/or PD-L1 downregulation inhibited the proliferation of H1299 cells. **C** Wound-healing assays showed that $\alpha$5-nAChR and/or PD-L1 downregula-tion inhibited the migration of A549 cells. **D** Wound-healing assays showed that $\alpha$5-nAChR and/or PD-L1 downregulation inhibited the migration of H1299 cells. The data are presented as the mean $\pm$ SD of independent experiments; $n = 3$; *$p < 0.05$, **$p < 0.01$, ***$p < 0.001$, ****$p < 0.0001$

## Discussion

Smoking represents the highest risk factor for the

development of lung cancer [32, 33]. Nicotine in ciga-rettes can induce addiction, and its derivatives become potent carcinogens after metabolic activation and activate
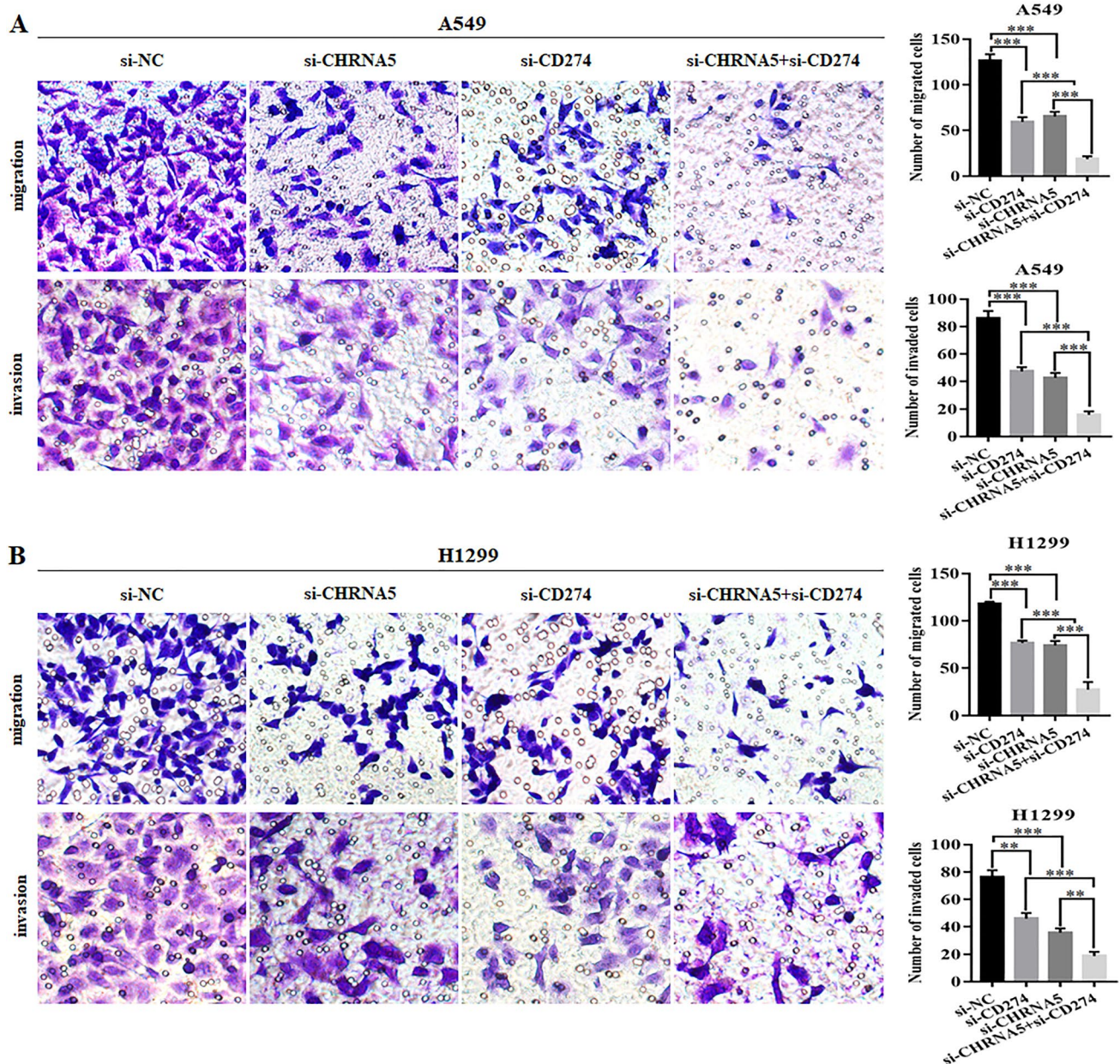
**Fig. 6** Downregulation of $\alpha$5-nAChR and/or PD-L1 affects lung cancer cell migration and invasion. **A** Transwell assays showed that $\alpha$5-nAChR and/or PD-L1 downregulation inhibited the migration and invasion of A549 cells. **B** Transwell assays showed that $\alpha$5-nAChR and/or PD-L1 downregulation inhibited the migration and invasion of H1299 cells. The data are presented as the mean $\pm$ SD of independent experiments; $n = 3$; **$p < 0.01$, ***$p < 0.001$

carcinogenic signals in lung epithelial cells through the expression of nAChRs [28]. Since genome-wide association studies have shown that CHRNA5 is highly associated with lung cancer susceptibility [34, 35], many investigators have begun to explore the role of nAChRs in the progression of different tumors. Studies have shown that nicotine and components of E-cigarettes can promote the self-renewal of lung adenocarcinoma stem-like cells through the $\alpha$7-nAChR–Yap1–E2F1 signaling axis [36].

The use of $\alpha$*-conotoxin to target $\alpha$9$\alpha$10 or $\alpha$3$\beta$4 nAChR significantly inhibits cervical cancer cell proliferation [37]. Binding immunoglobulin protein was shown to be involved in nicotine-mediated malignancy of oral squamous cell carcinoma, and reduction of binding immunoglobulin protein expression significantly suppressed nicotine-induced malignant behaviors, including EMT alterations, migration, and invasion [38]. However, previous studies have
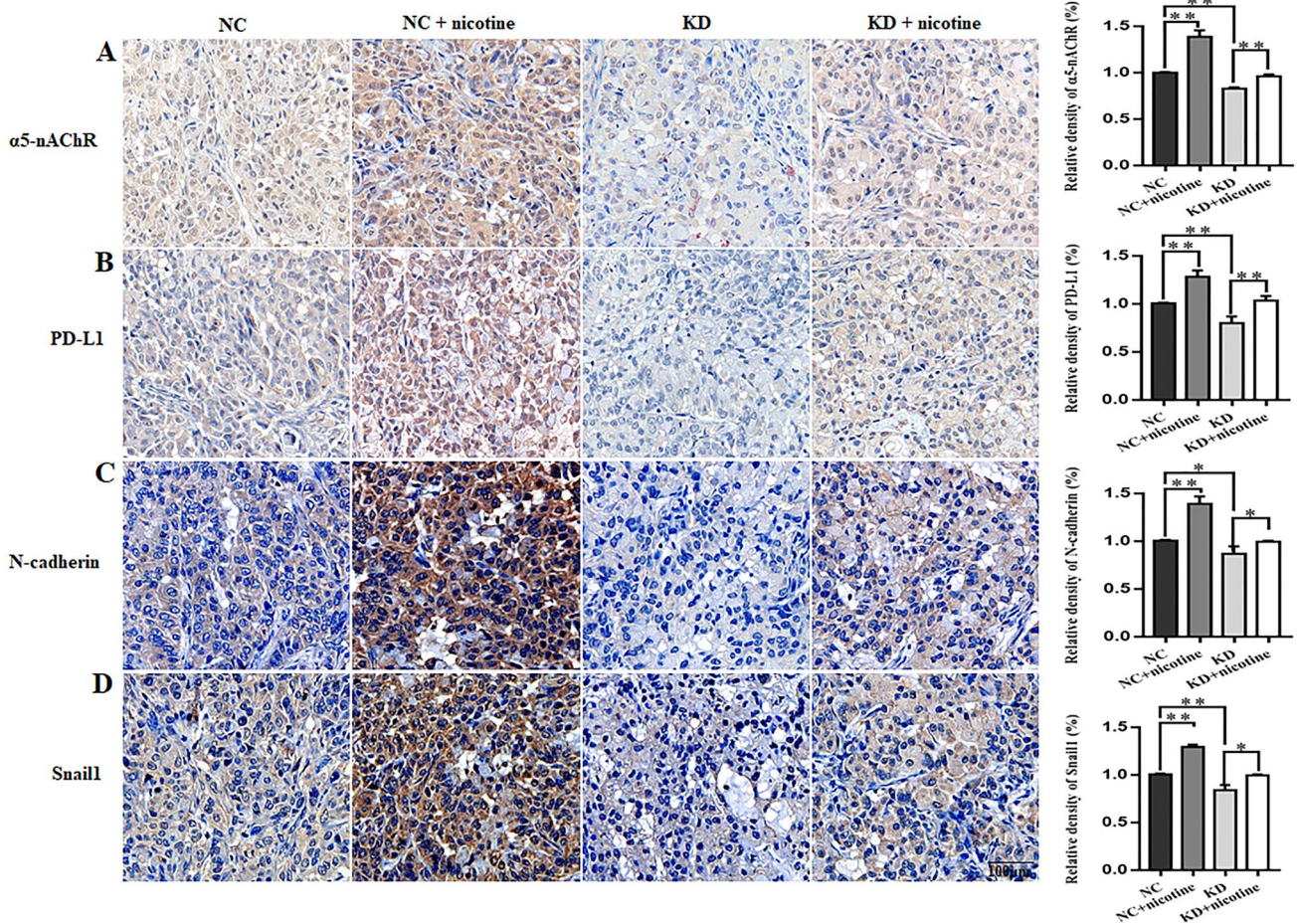
**Fig. 7** α5-nAChR, PD-L1, N-cadherin and Snail1 expression in LUAD tumor xenograft tissues. **A** The expression of α5-nAChR in various groups. **B** The expression of PD-L1 in various groups. **C** The expression of N-cadherin in various groups. **D** The expression of Snail1 in various groups. ×200, Scale bar, 100 μm. *KD* knockdown, *NC* normal control. The data are presented as the mean ± SD of independent experiments; *p* < 0.05, **p* < 0.01

focused on the carcinogenic mechanisms of various subunits in tumors other than lung cancer.

Notably, our previous studies reported that α5-nAChR mediates nicotine-induced lung cancer growth and development via the HIF-1α/VEGF and JAK2/STAT3 pathways. Our studies have also demonstrated that α5-nAChR contributes to epithelial–mesenchymal transition and metastasis by regulating Jab1/Csn5 and TGF-β1/Smad signaling in lung cancer. Taken together, these findings suggest a positive role of α5-nAChR in NSCLC tumor progression.

Numerous findings have indicated that PD-L1 is highly expressed in tumor cells [39]. PD-L1 binds to its receptor PD-1 on activated T cells and suppresses antitumor immunity by inhibiting T cell activation signals [40–42]. However, PD-L1 not only plays a role in facilitating tumor cells from escaping immune surveillance, but is also considered to be an important effector that transmits intrinsic signals to promote tumor development [43]. Inhibition of STAT1 and

STAT3 activation alone can partially downregulate PD-L1 expression, while the combined inhibition of these factors can completely downregulate PD-L1 expression [44]. In addition, STAT3 binds to the PD-L1 gene promoter and mediates PD-L1 expression in vitro [45]. Nevertheless, the link between α5-nAChR and PD-L1 in metastatic lung cancer is unclear.

In this study, the expression of α5-nAChR and PD-L1 was significantly associated with metastasis and poor prognosis in LUAD patients. α5-nAChR played roles in regulating LUAD cell proliferation, migration and invasion via STAT3/PD-L1 signaling pathways.

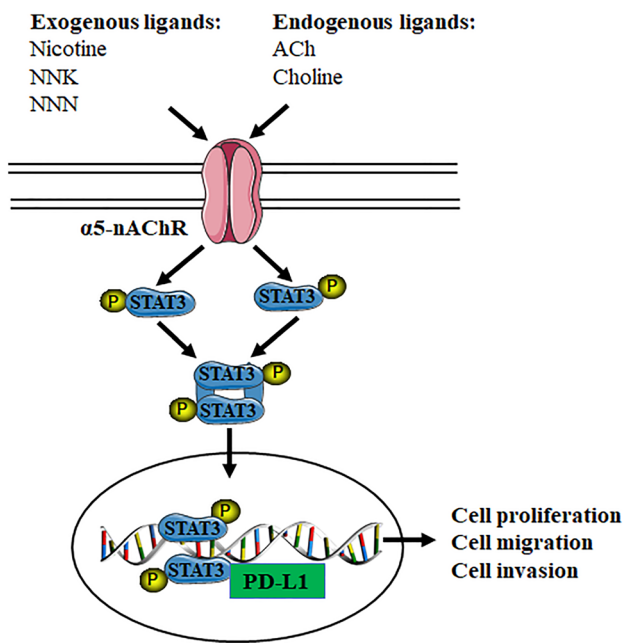**Fig. 8** Proposed signaling cascades of α5-nAChR and PD-L1 involved in metastasis in lung cancer. Nicotine binds and interacts with α5-nAChR on the cell surface and activates STAT3/PD-L1 signaling, thereby mediating lung cancer progression through the α5-nAChR/PD-L1 axis

## Conclusions

In conclusion, these findings provide experimental evidence of the mechanisms underlying lung cancer progression through α5-nAChR-initiated carcinogenic signaling and PD-L1 expression. Nicotine binds and interacts with α5-nAChR on the cell surface and activates STAT3/PD-L1 signaling, which subsequently mediates lung cancer progression (Fig. 8). α5-nAChR could be a potential marker and therapeutic target for predicting the risk of LUAD patients.

## Declarations

## References

1. Siegel RL, Miller KD, Fuchs HE, Jemal A. Cancer statistics. CA Cancer J Clin. 2021. https://doi.org/10.3322/caac.21654.
2. Heron M, Anderson RN. Changes in the leading cause of death: recent patterns in heart disease and cancer mortality. NCHS Data Brief. 2016;254:1–8.
3. Rojewski AM, Tanner NT, Dai L, et al. Tobacco dependence predicts higher lung cancer and mortality rates and lower rates of smoking cessation in the national lung screening trial. Chest. 2018;154:110–8. https://doi.org/10.1016/j.chest.2018.04.016.
4. Friedlaender A, Addeo A, Russo A, Gregorc V, Cortinovis D, Rolfo CD. Targeted therapies in early stage NSCLC: hype or hope? Int J Mol Sci. 2020. https://doi.org/10.3390/ijms21176329.
5. Herbst RS, Morgensztern D, Boshoff C. The biology and management of non-small cell lung cancer. Nature. 2018;553:446–54. https://doi.org/10.1038/nature25183.
6. Kim BN, Ahn DH, Kang N, et al. TGF-β induced EMT and stemness characteristics are associated with epigenetic regulation in lung cancer. Sci Rep. 2020;10:10597. https://doi.org/10.1038/s41598-020-67325-7.
7. Zhang N, Ng AS, Cai S, Li Q, Yang L, Kerr D. Novel therapeutic strategies: targeting epithelial-mesenchymal transition in colorectal cancer. Lancet Oncol. 2021;22:e358–68. https://doi.org/10.1016/S1470-2045(21)00343-0.
8. Lam DCL, Girard L, Ramirez R, et al. Expression of nicotinic acetylcholine receptor subunit genes in non-small-cell lung cancer reveals differences between smokers and nonsmokers. Cancer Res. 2007;67(10):4638–47.
9. Cheng W-L, Chen K-Y, Lee K-Y, Feng P-H, Wu S-M. Nicotinic-nAChR signaling mediates drug resistance in lung cancer. J Cancer. 2020;11:1125–40. https://doi.org/10.7150/jca.36359.
10. Benowitz NL. Nicotine addiction. N Engl J Med. 2010;362:2295–303. https://doi.org/10.1056/NEJMra0809890.
11. Zhou W, Zhu W, Tong X, et al. CHRNA5 rs16969968 polymorphism is associated with lung cancer risk: a meta-analysis. Clin Respir J. 2020;14:505–13. https://doi.org/10.1111/crj.13165.
12. Yao C, Joehanes R, Wilson R, et al. Epigenome-wide association study of whole blood gene expression in framingham heart study participants provides molecular insight into the potential role of CHRNA5 in cigarette smoking-related lung diseases. Clin Epigenetics. 2021;13:60. https://doi.org/10.1186/s13148-021-01041-5.
13. Hung RJ, McKay JD, Gaborieau V, et al. A susceptibility locus for lung cancer maps to nicotinic acetylcholine receptor subunit

genes on 15q25. Nature. 2008;452:633–7. https://doi.org/10.1038/nature06885.

14. Wen L, Jiang K, Yuan W, Cui W, Li MD. Contribution of variants in CHRNA5/A3/B4 gene cluster on chromosome 15 to tobacco smoking: from genetic association to mechanism. Mol Neurobiol. 2016;53:472–84. https://doi.org/10.1007/s12035-014-8997-x.

15. Zhang Q, Jia Y, Pan P, et al. $\alpha$5-nAChR associated with Ly6E modulates cell migration via TGF-$\beta$1/Smad signaling in non-small cell lung cancer. Carcinogenesis. 2022. https://doi.org/10.1093/carcin/bgac003.

16. Chen X, Jia Y, Zhang Y, Zhou D, Sun H, Ma X. $\alpha$5-nAChR contributes to epithelial-mesenchymal transition and metastasis by regulating Jab1/Csn5 signalling in lung cancer. J Cell Mol Med. 2020;24:2497–506. https://doi.org/10.1111/jcmm.14941.

17. Zhang Y, Jia Y, Li P, et al. Reciprocal activation of $\alpha$5-nAChR and STAT3 in nicotine-induced human lung cancer cell proliferation. J Genet Genomics. 2017;44:355–62. https://doi.org/10.1016/j.jgg.2017.03.003.

18. Ishida Y, Agata Y, Shibahara K, Honjo T. Induced expression of PD-1, a novel member of the immunoglobulin gene superfamily, upon programmed cell death. EMBO J. 1992;11:3887–95.

19. Sun C, Mezzadra R, Schumacher TN. Regulation and function of the PD-L1 checkpoint. Immunity. 2018;48:434–52. https://doi.org/10.1016/j.immuni.2018.03.014.

20. Latchman Y, Wood CR, Chernova T, et al. PD-L2 is a second ligand for PD-1 and inhibits T cell activation. Nat Immunol. 2001;2:261–8.

21. Mi Y, Han J, Zhu J, Jin T. Role of the PD-1/PD-L1 signaling in multiple sclerosis and experimental autoimmune encephalomyelitis: recent insights and future directions. Mol Neurobiol. 2021;58:6249–71. https://doi.org/10.1007/s12035-021-02495-7.

22. Zhang M, Li G, Wang Y, et al. PD-L1 expression in lung cancer and its correlation with driver mutations: a meta-analysis. Sci Rep. 2017;7:10255. https://doi.org/10.1038/s41598-017-10925-7.

23. Li JJN, Karim K, Sung M, et al. Tobacco exposure and immunotherapy response in PD-L1 positive lung cancer patients. Lung Cancer. 2020;150:159–63. https://doi.org/10.1016/j.lungcan.2020.10.023.

24. Li B, Huang X, Fu L. Impact of smoking on efficacy of PD-1/PD-L1 inhibitors in non-small cell lung cancer patients: a meta-analysis. Onco Targets Ther. 2018;11:3691–6. https://doi.org/10.2147/OTT.S156421.

25. Zaleskis G, Pasukoniene V, Characiejus D, Urbonas V. Do the benefits of being a smoker hint at the existence of PD-1/PD-L1 sensitizers for patients on single-agent immunotherapy? J Immunother Cancer. 2021. https://doi.org/10.1136/jitc-2021-003191.

26. Dong P, Xiong Y, Yue J, Hanley SJB, Watari H. Tumor-intrinsic PD-L1 signaling in cancer initiation, development and treatment: beyond immune evasion. Front Oncol. 2018;8:386. https://doi.org/10.3389/fonc.2018.00386.

27. Nguyen HD, Liao Y-C, Ho Y-S, et al. The $\alpha$9 nicotinic acetylcholine receptor mediates nicotine-induced PD-L1 expression and regulates melanoma cell proliferation and migration. Cancers. 2019. https://doi.org/10.3390/cancers11121991.

28. Kwok HH, Gao B, Chan KH, Ip MSM, Minna JD, Lam DCL. Nicotinic acetylcholine receptor subunit $\alpha$7 mediates cigarette smoke-induced PD-L1 expression in human bronchial epithelial cells. Cancers. 2021. https://doi.org/10.3390/cancers13215345.

29. Ma X, Jia Y, Zu S, et al. $\alpha$5 Nicotinic acetylcholine receptor mediates nicotine-induced HIF-1$\alpha$ and VEGF expression in non-small cell lung cancer. Toxicol Appl Pharmacol. 2014;278:172–9. https://doi.org/10.1016/j.taap.2014.04.023.

30. Sun H-J, Jia Y-F, Ma X-L. $\alpha$5 nicotinic acetylcholine receptor contributes to nicotine-induced lung cancer development and progression. Front Pharmacol. 2017;8:573. https://doi.org/10.3389/fphar.2017.00573.

31. Cao L, Wang X, Li S, et al. PD-L1 is a prognostic biomarker in resected NSCLC patients with moderate/high smoking history and elevated serum SCCA level. J Cancer. 2017;8:3251–60. https://doi.org/10.7150/jca.21118.

32. Bracken-Clarke D, Kapoor D, Baird AM, et al. Vaping and lung cancer: a review of current data and recommendations. Lung Cancer. 2021;153:11–20. https://doi.org/10.1016/j.lungcan.2020.12.030.

33. Dela Cruz CS, Tanoue LT, Matthay RA. Lung cancer: epidemiology, etiology, and prevention. Clin Chest Med. 2011;32:605–44. https://doi.org/10.1016/j.ccm.2011.09.001.

34. Amos CI, Wu X, Broderick P, et al. Genome-wide association scan of tag SNPs identifies a susceptibility locus for lung cancer at 15q25.1. Nat Genet. 2008;40:616–22.

35. Liu JZ, Tozzi F, Waterworth DM, et al. Meta-analysis and imputation refines the association of 15q25 with smoking quantity. Nat Genet. 2010;42:436–40. https://doi.org/10.1038/ng.572.

36. Schaal CM, Bora-Singhal N, Kumar DM, Chellappan SP. Regulation of Sox2 and stemness by nicotine and electronic-cigarettes in non-small cell lung cancer. Mol Cancer. 2018;17:149. https://doi.org/10.1186/s12943-018-0901-2.

37. Liu Y, Qian J, Sun Z, Zhangsun D, Luo S. Cervical cancer correlates with the differential expression of nicotinic acetylcholine receptors and reveals therapeutic targets. Mar Drugs. 2019. https://doi.org/10.3390/md17050256.

38. Chien CY, Chen YC, Hsu CC, et al. YAP-dependent BiP induction is involved in nicotine-mediated oral cancer malignancy. Cells. 2021. https://doi.org/10.3390/cells10082080.

39. Wang Y, Wang H, Yao H, Li C, Fang J-Y, Xu J. Regulation of PD-L1: emerging routes for targeting tumor immune evasion. Front Pharmacol. 2018;9:536. https://doi.org/10.3389/fphar.2018.00536.

40. Dermani FK, Samadi P, Rahmani G, Kohlan AK, Najafi R. PD-1/PD-L1 immune checkpoint: potential target for cancer therapy. J Cell Physiol. 2019;234:1313–25. https://doi.org/10.1002/jcp.27172.

41. Wu Y, Chen W, Xu ZP, Gu W. PD-L1 distribution and perspective for cancer immunotherapy-blockade, knockdown, or inhibition. Front Immunol. 2019;10:2022. https://doi.org/10.3389/fimmu.2019.02022.

42. Yi M, Niu M, Xu L, Luo S, Wu K. Regulation of PD-L1 expression in the tumor microenvironment. J Hematol Oncol. 2021;14:10. https://doi.org/10.1186/s13045-020-01027-5.

43. Du W, Zhu J, Zeng Y, et al. KPNB1-mediated nuclear translocation of PD-L1 promotes non-small cell lung cancer cell proliferation via the Gas6/MerTK signaling pathway. Cell Death Differ. 2021;28:1284–300. https://doi.org/10.1038/s41418-020-00651-5.

44. Sasidharan Nair V, Toor SM, Ali BR, Elkord E. Dual inhibition of STAT1 and STAT3 activation downregulates expression of PD-L1 in human breast cancer cells. Expert Opin Ther Targets. 2018;22:547–57. https://doi.org/10.1080/14728222.2018.1471137.

45. Song TL, Nairismägi M-L, Laurensia Y, et al. Oncogenic activation of the STAT3 pathway drives PD-L1 expression in natural killer/T-cell lymphoma. Blood. 2018;132:1146–58. https://doi.org/10.1182/blood-2018-01-829424.